



Singaporean Journal of Scientific Research(SJSR)  
Journal of Selected Areas in Microelectronics (JSAM)  
Vol.8.No.2 2016 Pp.101-107  
available at :www.iaaet.org/sjsr  
Paper Received : 08-03-2016  
Paper Accepted: 19-04-2016  
Paper Reviewed by: 1.Prof. Cheng Yu 2. Dr.M. Akshay Kumar  
Editor : Dr. Chu Lio

---

**CONTINUOUS CONDUCTION MODE USING SOFT  
SWITCHING BOOST CONVERTER WITH HIGH VOLTAGE  
GAIN FOR THE LARGE POWER APPLICATION**

**P.Sakthivel**  
PG Scholar  
Electrical and Electronics  
Engineering  
Salem,Tamilnadu, india

**Dr.P.Karpagavalli**  
Assistant Professor  
Electrical and Electronics  
Engineering  
Salem, Tamilnadu, india

---

**ABSTRACT**

This paper proposes a new soft-switched continuous conduction-mode (CCM) boost converter. its suitable for high-power applications such as hybrid electric vehicles, and fuel cell power conversion systems. The proposed converter achieves zero-voltage-switched (ZVS) turn-on of active switches in CCM and zero-current-switched turn-off of diodes leading to negligible reverse-recovery loss. The components voltage ratings and energy volumes of passive components of the proposed converter are greatly reduced compared to the conventional zero-voltage-transition converter. Voltage conversion ratio is almost doubled compared to the conventional converter. Extension of the proposed concept to realize multiphase dc–dc converters is discussed.

---

**Index Terms**—*Continuous conduction mode(CCM),high-power systems, high voltage gain, soft switched.*

---

**I. INTRODUCTION**

CONTINUOUS-conduction-mode(CCM)boost converters have been widely used as the front-end converter .In recent years, CCM boost converters are increasingly needed in high-power applications such as hybrid electric vehicles and fuel cell power conversion systems. High power density and high

efficiency are major concerns in high-power CCM boost converters[1],[2]

The hard-switched CCM boost converter suffers from severe diode reverse-recovery problem in high-current high-power applications. That is, when the main switch is turned on, a shoot through of the output capacitor to ground due to the diode reverse recovery causes a large current spike through

the diode and main switch. This not only incurs significant turn-off loss of the diode and turn-on loss of the main switch, but also causes severe electromagnetic interference (EMI) emission. The effect of the reverse-recovery-related problems become more significant for high switching frequency at high power level. Therefore, the hard-switched CCM boost converter is not capable to achieve high efficiency.

The zero-voltage switched (ZVS) quasi resonant converter (QRC) achieves soft switching of the main switch with ZVS and the diode with zero current switched (ZCS), but both main switch and diode suffer from an excessive voltage stress due to resonant operation[2][4][6] The ZVS quasi square-wave converter (QSW) technique offers ZVS turn-on for both main switch and diode without increasing their voltage stresses. However, both main switch and diode suffer from a high current stress resulting in significant conduction losses. Furthermore, turn-off loss of the main switch is considerable. Since both ZVS-QRC and ZVS-QSW techniques achieve soft switching only at the expense of increased conduction losses due to voltage or current stresses of the components, they are not suitable for high-power applications[10].

The zero-voltage-transition (ZVT) pulse width modulation (PWM) converter[6] achieves soft switching of the main switch and diode without increasing their voltage or current stresses, since ZVS is achieved by partial resonance of the shunt branch across the main switch. Furthermore, the reverse recovery-related problem is alleviated by controlling diode current decrease rate  $di/dt$  during its turn off. However, severe undesired resonance may occur in the shunt branch. Adding a rectifier and saturable inductor can mitigate the resonance, but this causes circuit complexity and additional cost[5]. Also, the auxiliary switch in the shunt branch is hard switched, and the duty ratio of the auxiliary switch limits the effective duty ratio of the main switch, leading to decreased voltage conversion ratio of the converter.

This paper proposes a new soft-switched CCM boost converter suitable for high-power applications such as hybrid electric vehicles, and fuel cell power conversion systems. The proposed converter has the following advantages:

- 1) ZVS turn-on of the main switches in CCM;
- 2) negligible diode reverse recovery due to ZCS turn-off of the diode;
- 3) voltage conversion ratio is almost doubled compared to the conventional boost converter;
- 4) significantly reduced components' voltage ratings and energy volumes of most passive components.

## II. PROPOSED SOFT-SWITCHED BOOST CONVERTER

Fig. 1 shows the circuit diagram of the proposed CCM boost converter[7], and Fig. 2 shows key waveforms illustrating the operating principle of the proposed converter. Upper switch  $S_2$  in the proposed converter replaces the rectifier diode in the conventional boost converter. Lower switch  $S_1$  and upper switch

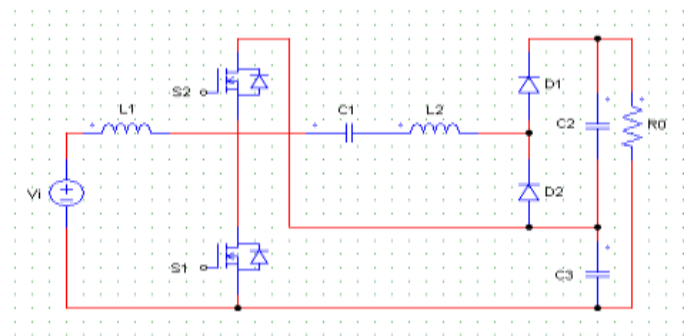


**Fig. 1. Proposed soft-switched CCM boost converter.**

$S_2$  are operated with asymmetrical complementary switching to regulate the output voltage as shown in Fig. 2. An auxiliary circuit that consists of a capacitor  $C_1$ , an inductor  $L_2$ , two diodes  $D_1$  and  $D_2$ , and a capacitor  $C_2$  is connected on top of the output capacitor  $C_3$  to form the output voltage of the converter. The auxiliary circuit not only increases the output voltage, but also helps

ZVS turn-on of active switches  $S_1$  and  $S_2$  in CCM.

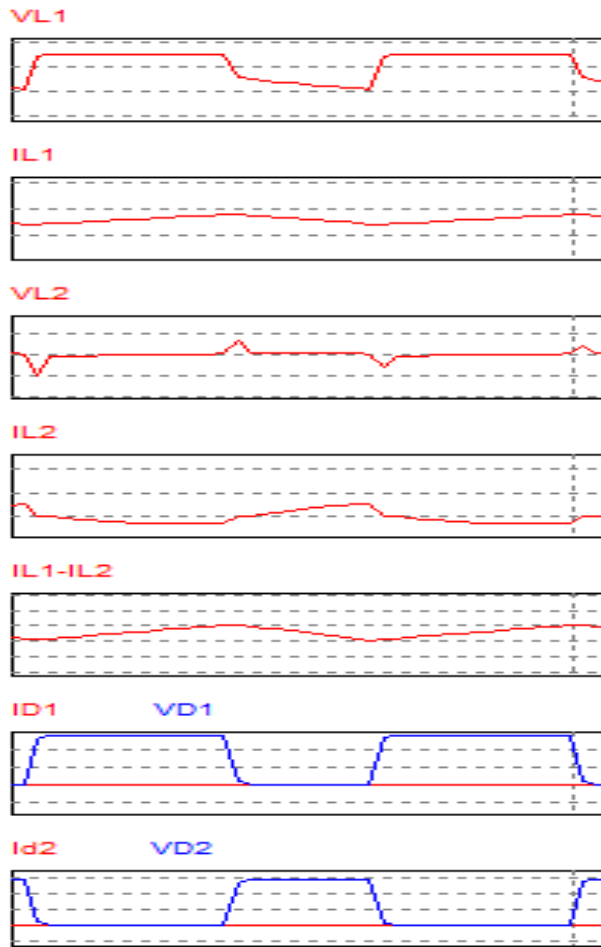


**Fig. 2. Theoretical Key waveforms of the proposed converter.**

### A. Operating Principle

As shown in Fig. 2, the operation of the proposed converter can be divided into five modes. The equivalent circuits for each mode are shown in Fig. 3.

*Mode I:* This mode begins when  $i_{L2}$  decreases to zero and  $D_2$  is turned on as shown in Fig. 2. During this mode, the lower switch  $S_1$  maintains ON state. Both input inductor current  $i_{L1}$  and auxiliary inductor current  $i_{L2}$  flows through lower switch  $S_1$ . The slope of these currents are given by

$$\frac{di_{L1}}{dt} = \frac{V_i}{L_1} \quad (1)$$

$$\frac{di_{L2}}{dt} = \frac{(V_{c1}-V_{c3})}{L_2} \quad (2)$$

*Mode II:* This mode begins when  $S_1$  is turned off and the body diode of  $S_2$  is turned on. The gating signal for  $S_2$  is applied during this mode, and  $S_2$  is turned on under ZVS conditions. Both  $i_{L1}$  and  $i_{L2}$  are decreasing with the slope determined by the following equations:

$$\frac{di_{L1}}{dt} = \frac{(V_i-V_{c3})}{L_1} \quad (3)$$

$$\frac{di_{L2}}{dt} = \frac{V_{c1}}{L_2} \quad (4)$$

At the end of this mode, inductor current  $i_{L2}$  changes its direction of flow and  $D_1$  starts to conduct. It should be noted that  $D_2$  is turned off under ZCS.

*Mode III:* During this mode,  $i_{L1}$  keeps decreasing with the slope determined in Mode II, and  $i_{L2}$  increases with slope determined by the following equation:

$$\frac{di_{L2}}{dt} = \frac{(V_{c1}-V_{c2})}{L_2} \quad (5)$$

At the end of this mode, switch current  $i_{S2}$  reverses its direction of flow and conducts the main channel of  $S_2$ .

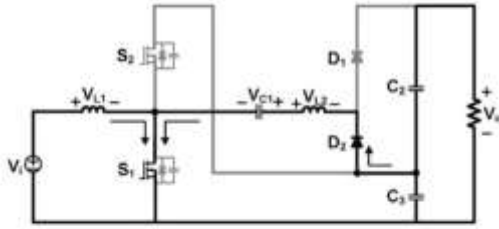
*Mode IV:* During this mode,  $i_{L1}$  and  $i_{L2}$  keep flowing with the same slope determined in Mode III.

*Mode V:* This mode begins when  $S_2$  is turned off and the body diode of  $S_1$  is turned on. The gating signal for  $S_1$  is applied during this mode, and  $S_1$  could be turned on under ZVS conditions. Inductor currents  $i_{L1}$  and  $i_{L2}$  start to increase and decrease, respectively, with the slope determined by the following equations:

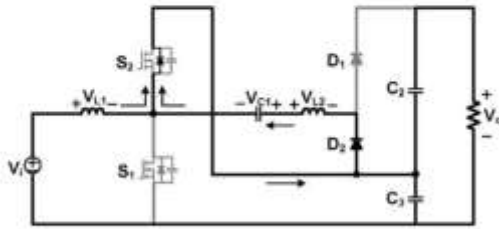
$$\begin{aligned} & \frac{di_{L1}}{dt} \\ &= \frac{V_i}{L_1} \\ & \frac{di_{L2}}{dt} \\ &= \frac{(V_{c1}-V_{c2}-V_{c3})}{L_2} \end{aligned} \quad (6) \quad (7)$$

This state ends when the decreasing current  $i_{L2}$  reaches to 0 V. This is the end of one complete cycle. Note that diode  $D_1$  is also turned off under ZCS.

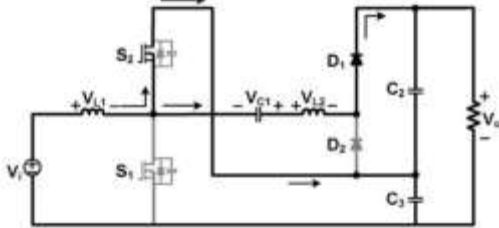
Mode 1



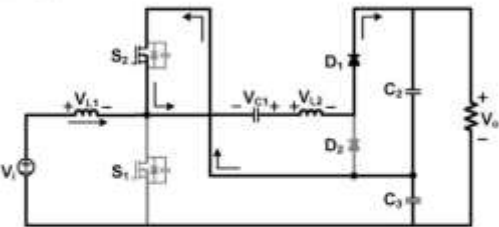
Mode 2



Mode 3



Mode 4



Mode 5

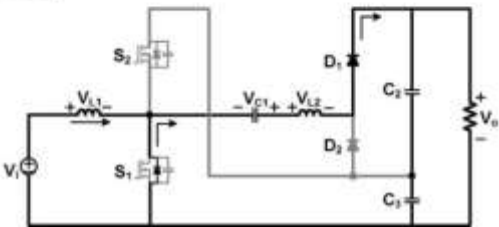


Fig. 3. Operation modes of the proposed converter.

**B. Voltage Conversion Ratio**

To obtain the voltage gain of the proposed converter, it is assumed that the voltage across  $C_1, C_2$ , and  $C_3$  are constant during the switching period of  $T_s$ . The output voltage is given by

$$V_o = V_{C2} + V_{C3} \quad (8)$$

$$V_o = \frac{2}{1-D} V_i - \Delta V \quad (9)$$

where the effective duty  $D_{eff}$  is defined by

$$D_{eff} = D + M_1 - M_2. \quad (10)$$

The output voltage can also be expressed as

$$V_o = \frac{2}{1-D} V_i - \Delta V \quad (11)$$

where  $\Delta V$  is the voltage drop caused by the duty loss  $(M_2 - M_1)$ . From (9)–(11), the voltage drop  $\Delta V$  can be obtained by

$$\Delta V = \frac{2V_i(M_2 - M_1)}{(1 - D)(1 - D + M_2 - M_1)} \quad (12)$$

According to volt-sec balance principle on  $L_2$ , capacitor voltage  $V_{C1}$  can be obtained by

$$V_{C1} = V_{C2} (1 - D - (M_2 - M_1)) + DV_{C3} \quad (13)$$

where  $V_{C2}$  and  $V_{C3}$  can be expressed as

$$V_{C3} = \frac{1}{1-D} V_i \quad (14)$$

$$V_{C2} = \frac{1}{1-D} V_i - \Delta V \quad (15)$$

In the steady state, the average output load current equals the average current of  $D_1$  and  $D_2$  since the average value of the current through  $L_2(C_2)$  is zero. The following equations can be derived:

$$I_{D1,av} = \frac{V_o}{R_o} = \frac{1}{2}(1 - D - (M_2 - M_1))I_{L2,+pk} \quad (16)$$

$$I_{D2,av} = \frac{V_o}{R_o} = \frac{1}{2}(D + M_2 - M_1)I_{L2,-pk} \quad (17)$$

where  $I_{L2,+pk}$  and  $I_{L2,-pk}$  are positive and negative peak values of the inductor current  $I_{L2}$ , and are given by (see Fig. 2)

$$I_{L2+PK} = \frac{(V_{C1} - V_{C2} - V_{C3})M_1T_s}{L_2} \quad (18)$$

$$I_{L2-PK} = \frac{V_{C1}M_2T_S}{L_2} \quad (19)$$

Diode current  $I_{D2}$ , which is a negative portion of current  $I_{L2}$ , becomes incremental current in switch  $S_1$ , resulting in increased conduction loss. At the same time, diode current  $I_{D1}$ , which is a positive portion of current  $I_{L2}$ , becomes decremental current in switch  $S_2$ , resulting in decreased conduction loss.

Also, current  $I_{L2}$  increases the ZVS currents for both lower switch,  $I_{S1,ZVS}$ , and upper switch,  $I_{S2,ZVS}$ , resulting in reduced switching losses. The peak values  $I_{L2,-pk}$  and  $I_{L2,+pk}$  can be adjusted by the inductance  $L_2$ . Therefore, the magnitude of current  $I_{L2}$  should be properly designed considering this tradeoff relation.

Using equation (11)-(19) The effective voltage gain of the proposed converter is plotted as shown in Fig. 4. Even though there is a slight drop of the ideal voltage gain, which is caused by duty loss ( $M_2-M_1$ ), the effective voltage gain of the proposed converter is almost twice compared to that of the conventional boost

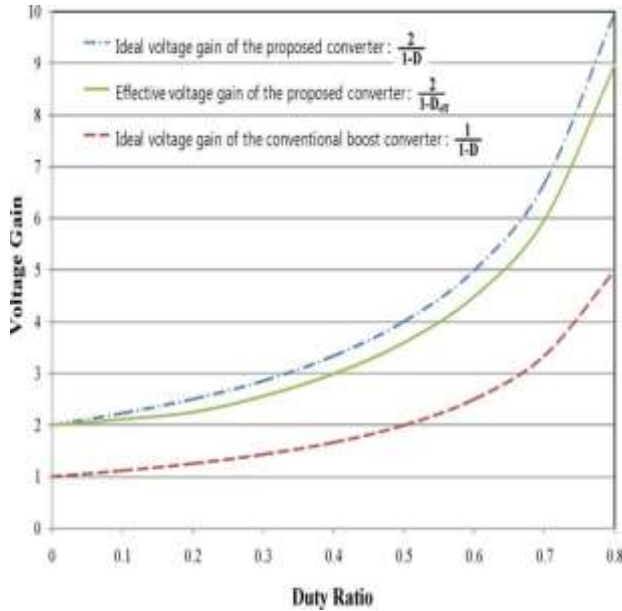


**Fig. 4. Voltage gain as a function of duty ratio ( $V_i = 80$  V,  $L_2 = 7 \mu\text{H}$ ,  $f_s = 70$  kHz,  $P_o = 1.5$  kW).**

converter. This is a very desirable feature in high-voltage-gain application since reduced duty ratio leads to reduced current stresses on the components resulting in increased

efficiency. Duty loss ( $M_2-M_1$ ) can be reduced by choosing smaller inductance  $L_2$ , but this reduces ZVS range of main switch  $S_1$ . Therefore, inductance  $L_2$  should be properly chosen, considering a tradeoff of switching loss and voltage gain.

### C. ZVS Characteristic for Main Switch

ZVS of the upper and lower switches depends on the difference of the filter inductor current  $i_{L1}$  and auxiliary inductor current  $i_{L2}$ , as shown in Fig. 2. The ZVS current for lower switch  $I_{S1,ZVS}$  is the positive peak of  $i_{L1} - i_{L2}$  when the upper switch is turned off and can be expressed as

$$I_{S1,ZVS} = IL_{2,+pk} - IL_{1,min} \\ = \frac{(V_{C1} - V_{C2} - V_{C3})M_1T_S}{L_2} - \left( \frac{V_0^2}{V_i R_o} + \frac{DV_i}{2L_1f_s} \right) \quad (20)$$

The ZVS current for upper switch  $I_{S2,ZVS}$  is the negative peak of  $i_{L1} - i_{L2}$  when the lower switch is turned off and can be expressed as

$$I_{S2,ZVS} = |IL_{2,-pk}| + IL_{1,max} \\ = \frac{V_{C1}M_2T_S}{L_2} + \left( \frac{V_0^2}{V_i R_o} + \frac{DV_i}{2L_1f_s} \right) \quad (21)$$

To ensure the ZVS turn-on of upper switch  $S_2$ , the following condition should be satisfied:

$$\frac{1}{2}(L_1I_{L1,max}^2 + L_2I_{L2,-pk}^2) > \frac{1}{2}(C_{os1} + C_{os2})\left(\frac{V_i}{1-D}\right)^2 \quad (22)$$

where  $C_{os1}$  and  $C_{os2}$  are the output capacitances of lower switch  $S_1$  and upper switch  $S_2$ , respectively.

In fact, the condition of (22) can be easily satisfied, and ZVS of upper switch  $S_2$  can be achieved over the whole load range. To ensure the ZVS turn-on of lower switch  $S_1$ , the following condition should be satisfied:

$$\frac{1}{2}(L_2I_{L2,+pk}^2 - L_1I_{L1,min}^2) \\ > \frac{1}{2}(C_{os1} + C_{os2})\left(\frac{V_i}{1-D}\right)^2 \quad (23)$$

Equation (23) may not be satisfied under the conditions of small auxiliary inductance  $L_2$ , large input filter inductance  $L_1$ , and/or light load. Increasing auxiliary inductance  $L_2$  to enlarge the ZVS region makes the duty loss ( $M_2-M_1$ ) large. Alternatively, in order to enlarge the ZVS region, the input inductance can be decreased so that  $I_{S1,ZVS}$  can be increased. However, decreasing the input filter inductance increases the current rating of the power devices, and therefore the input filter inductance should be properly chosen considering a tradeoff between the ZVS region and the device current ratings. Therefore, ZVS for lower switch  $S_1$  can be achieved more easily with smaller value of  $L_1$  and/or larger value of  $L_2$  at the cost of the large current ripple.

Using the ZVS current of the lower switch tends to increase as the output power increases and decrease as the voltage gain increases. This means that the ZVS turn-on of the lower switch can be more easily achieved under the condition of higher output power and lower voltage gain. It is noted that the ZVS range of the lower switch becomes broader for smaller total output capacitance  $C_{os,tot} = C_{os1}+C_{os2}$  of MOSFETs.

**D. Comparison of Component Ratings**

In order to perform a comparison of the proposed converter to the conventional ZVT converter [10] in terms of the component rating, the converters have been designed according to the following specifications:

- 1)  $P_o = 13$  kW.
- 2)  $V_i = 250$  V.
- 3)  $V_o = 600$  V.
- 4)  $\Delta I_i = 10$  %.
- 5)  $\Delta V_o = 3$  %.
- 6)  $f_s = 15$  kHz.

The component ratings of the proposed converter and the ZVT converter calculated according to the design specification are listed in Table I. Because of the proposed connection of the auxiliary circuit, the voltage ratings of all components of the proposed converter are much smaller compared to those of the ZVT

converter that are the same as the output voltage .

**III. EXTENSION OF THE PROPOSED CONCEPT**

Using the converter shown in Fig. 1 as a basic cell, the proposed concept can be extended to realize multiphase dc–dc converters for high-voltage and high-power applications. Fig. 6 shows the generalized circuit of the proposed multiphase dc–dc converter. The generalized converter has “ $N$ ” groups of converters, where each group of switch legs is connected in parallel at the low-voltage high-current side, while output capacitors in each group is connected in series at the high-voltage low current side. Each of the  $N$  groups also has “ $P$ ” parallel connected switch legs to increase the output power, where “ $P$ ” is the number of switch or diode legs connected to the same output capacitor.

**TABLE I**  
**Comparison Of Component Ratings Of The Proposed Converter And The ZVT Converter**

| Components          | Design items         | ZVT converter | Proposed converter |
|---------------------|----------------------|---------------|--------------------|
| Active switches     | Vph                  | 612v          | 387v               |
|                     | Iph                  | 6.53 A        | 15.6 A             |
|                     | Po/(Vpk.Ipk.q)       | 0.02          | 0.11               |
| Diodes              | Vph                  | 612v          | 223v               |
|                     | Iph                  | 5.2 A, 6.50 A | 10.1A              |
|                     | Po/(Vpk.Ipk.q)       | 0.03          | 0.3                |
| Output capacitor    | Capacitance          | 50 $\mu$ F    | 120 $\mu$ F        |
|                     | Vph                  | 612V          | 223V,387V          |
|                     | CV <sup>2</sup> (PU) | 1             | 1.3                |
| Input inductor      | Inductance           | 1400 $\mu$ H  | 1200 $\mu$ H       |
|                     | Irms                 | 5.2 A         | 5.2 A              |
|                     | LI <sup>2</sup> (PU) | 1             | 0.86               |
| Auxiliary capacitor | Capacitance          | 2 $\mu$ F     | 30 $\mu$ F         |
|                     | Irms                 | 9.8A          | 5A                 |
|                     | Vph                  | 612v          | 284v               |
|                     | CV <sup>2</sup> (PU) | 1             | 3.2                |
| Auxiliary inductor  | Inductance           | 2 $\mu$ H     | 25 $\mu$ H         |
|                     | Irms                 | 2.77A         | 5A                 |
|                     | LI <sup>2</sup> (PU) | 1             | 0.4                |

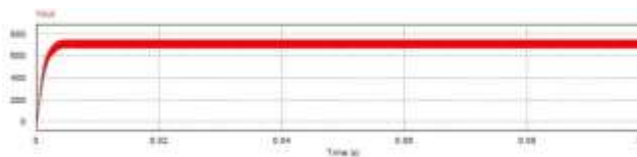
Fig. 5. Extension of the proposed concept for multiphase dc–dc converter .

Therefore, the switch and diode utilizations of the proposed converter are greatly improved. However, energy volumes of the other passive components are significantly reduced in the proposed converter. Input inductance of the proposed converter is smaller because the voltage across the inductor is smaller. Also, the current rating of the auxiliary inductor is much smaller compared to that of the ZVT converter, since the proposed converter does not utilize resonance while the ZVT converter utilizes partial resonance for soft switching.

#### IV EXPERIMENT RESULT

Simulation output using PSIM software

Output voltage



Output current

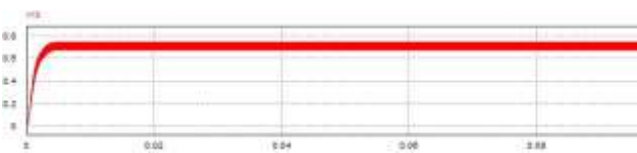


Fig. 6. Output voltage and output current

#### V. CONCLUSION

In this paper, a new soft-switched CCM boost converter suitable for high-voltage and high-power application has been proposed. The proposed converter has the following advantages:

- 1) zero voltage switching turn-on of the active switches in Continuous conduction mode.
- 2) negligible diode reverse recovery due to ZCS turn-off of the diodes.

- 3) voltage conversion ratio is almost doubled compared to the conventional boost converter.
- 4) greatly reduced components' voltage ratings and energy volumes of most passive components.

Extension of the proposed concept to realize multiphase dc– dc converters for higher voltage and higher power applications has been explored.

#### REFERENCES

- [1] V.Vorperian, "Quasi-square-wave converters: Topologies and analysis," *IEEE Trans. Power Electron.*, vol. 3, no. 2, pp. 183–191, Apr. 1988.
- [2] Q. Zhao, P. Xu, and F. C. Lee, "A simple and effective method to alleviate the rectifier reverse-recovery problem in continuous-current-mode boost converters," *IEEE Trans. Power Electron.*, vol. 16, no. 5, pp. 649–658, Sep. 2001
- [3] E. Ismail and A. Sebzali, "A new class of quasi-square wave resonant Converters with ZCS," in *Proc. IEEE APEC*, 1997, pp. 1381–1387.
- [4] G. Hua, C. Leu, and F. C. Lee, "Novel zero-voltage-transition PWM converters," in *Proc. IEEE PESC*, 1992, pp. 55–61
- [5] Q. Li and P. Wolfs, "An analysis of the ZVS two-inductor boost converter under variable frequency operation," *IEEE Trans. Power Electron.*, vol. 22, no. 1, pp. 120–131, Jan. 2007.
- [6] T.Mizoguchi, T.Ohgai, and T.Ninomiya, "A family of single-switch ZVS CV DC–DC converters," in *Proc. IEEE APEC*, 1994, vol. 2, pp. 1392 – 1398.
- [7] Sungsik park and sewan choi "soft switched boost converter for high power application" *IEEE trans, power Electron*, vol 25.no.5pp.1211,may 2010.
- [8] Power electronics by P.S.Bimphra, khanna publishers.